STACK GEOMETRY EFFECTS ON FLOW PATTERN WITH PARTICLE IMAGE VELOCIMETRY (PIV)

A. Irwan Shah, M. G. Normah[*], M. S. Jamaluddin, A. R. M. Aminullah and G. A. Dairobi

Faculty of Mechanical Engineering,
Universiti Teknologi Malaysia,
81310 Skudai, Johor Bahru

ABSTRACT

Thermoacoustic refrigerator system generates cooling power from acoustic energy. Acoustic waves interact with stack plates in the resonator tube of a thermoacoustic refrigerator to induce a temperature difference the significance of which depends on the solid-fluid interactions. In this paper, the flow field at the end of the stack plates was investigated using Particle Image Velocimetry (PIV). Results were obtained from three stack configurations with different plate geometry. Effects of plate thickness and separation gap were determined by comparison of the velocity profile obtained from these three configurations. The ratio of separation gaps to viscous penetration depth was also determined to see the effect of separation gaps. And for plate thickness effects, Reynolds number for each configuration was calculated.

Keywords: *Thermoacoustic, stack plates, particle image velocimetry (PIV), viscous penetration depth, reynolds number*

1.0 INTRODUCTION

Recently, considerations on the sustainability of our environment have become important issues in the design and development of new systems. The refrigeration industry has been pointed as one of the main causes of the ozone depletion issue, due to production of chlorofluorocarbons (CFC) which also contributes to the greenhouse effect. Thermoacoustic refrigerator, a system without CFC but uses inert gases instead, is an alternative to the conventional refrigeration system. Thermoacoustic is a combined phenomenon of acoustic and thermodynamics when pressure oscillations or acoustics generate a temperature gradient or vice versa.

The stack is considered as the heart of a thermoacoustic system. Development and continuous improvement of it can better the overall performance of a thermoacoustic system. The heat transfer process crucial to thermoacoustic effects occurs in and near the stack region. It was Carter *et al.* [1] who were responsible for introducing the stack in the thermoacoustic system. In 1992, to increase the thermoacoustic effects STAR thermoacoustic refrigeration system was developed using Mylar with spiral roll as the stack. This was the big turning point in stack development, as many researchers after that used Mylar as the stack material because of its success in generating greater cooling effects. The flow fields around the stack plates were generally measured using optical methods due to their non-intrusive characteristics. The visualization flow field techniques that have been used are Holographic Interferometry [2] and Laser Doppler Anemometry (LDA) [3][4]. However, these techniques only yield data for a single point in the measurement volume. A few researchers have used the Particle Image Velocimetry (PIV)

---

[*] Corresponding author : normah@fkm.utm.my

technique because it gives velocity data over a large area [5][6][7]. The experiments completed using this technique investigated vortex shedding processes occurring at the end of the stack of parallel plates due to the oscillating flow. They have shown the presence of vortices around thin and thick plates which affect the desired solid-fluid conductive heat transfer within the boundary layer regions.

This study involves an experimental analysis of flow around a thermoacoustic stack and also the effects of stack geometry on this flow field. Previous study has reported that the stack thickness and separation gap was not varied independently in their study. To determine the effect of stack geometry, the stack plate was fabricated with different thickness or separation gaps for different configurations. And the flow around the stack is visualized experimentally using PIV.

2.0   EXPERIMENTAL SETUP

The schematic illustration of thermoacoustic refrigerator used in this study is shown in Fig. 1. A resonator tube with length of 86 cm and cross sectional area of 80x80 mm^2 was filled with air at atmospheric pressure and the thermoacoustic stack consisted of glass plates. The walls of the resonator tube were fabricated using transparent acrylic material. The acoustic driver used was a loudspeaker at the resonance frequency of the resonator, $f = 200$ Hz (half-wavelength). Three stack configurations with different geometry were used in this study with length of each stack at 25 mm and width at 80 mm. The stack was placed in the resonator at 21.5 cm away from the driver where the amplitude for both pressure and velocity are high enough for the thermoacoustic effect to take place. Table 1 shows the geometry parameters for configuration A to C.
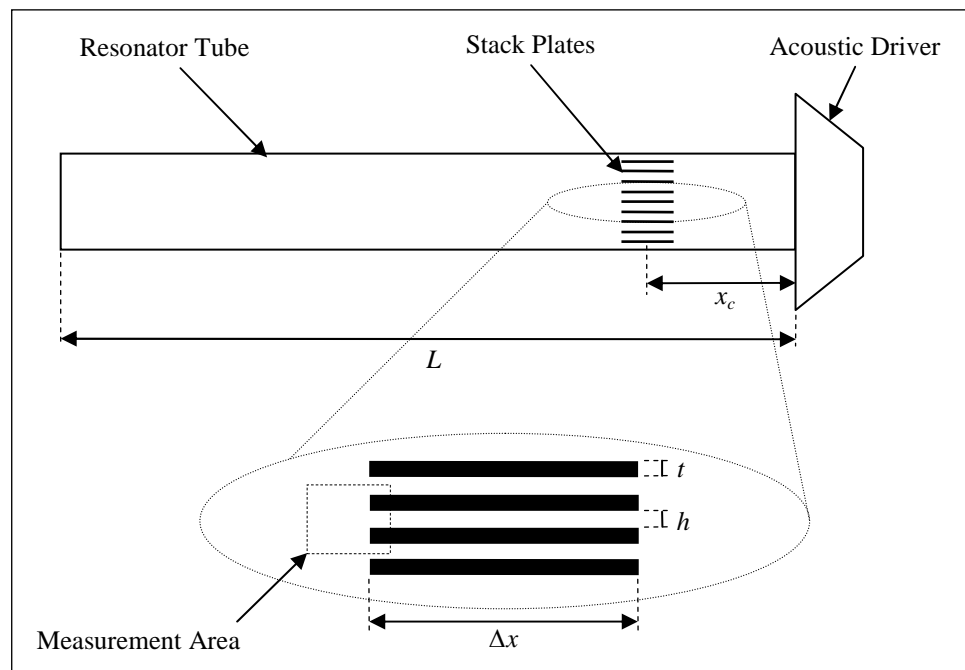

Figure1 : Schematic illustration of the thermoacoustic refrigerator with magnified view.

Table 1 : Geometry parameters for configuration A, B, and C.

	Stack Geometry (mm)				
	Thickness, t	Separation gap, h	Length, Δx	Width, w	Centre position, x_c
Configuration A	1	1	25	80	250
Configuration B	1	3	25	80	250
Configuration C	3	1	25	80	250

The flow fields around the stack plates were measured using PIV technique with flow inside the resonator seeded by a smoke generator located near the acoustic driver. An optical setup consists of Nd-YAG laser and CCD cameras were used to detect the flow patterns of the seeding particle. The area of velocity field was illuminated by a piece of light sheet in order to detect the movement while a camera was used to record the position of illuminated seeding particle. The working distance is approximately 10 cm from the measurement field. The camera was located perpendicular to the direction of oscillations and also perpendicular to the light sheet produced by laser. Both pulsing light sheet and camera were synchronized by using a flow manager software. Besides that, all data obtained from PIV measurement were also processed and analyzed using a flow manager software. The images of velocity profile were sent to a computer after being captured by the camera to give raw vector map. However, almost all PIV measurements may give an incorrect vectors resulting from noise peak in the correlation function called outlier. Therefore, PIV raw vector map was validated to recognize, reject and remove this outlier. Vector map was also filtered out to reduce the effect of noise which gives rise to small errors.

3.0   RESULTS AND DISCUSSION

The results are focused only on one side of the stack which is far from the acoustic driver. In order to perform a comparison between the configurations, it was necessary to properly synchronized the time axes. For all three configurations, data analysis was performed at the same time. The PIV measurement was started 6 seconds after the acoustic driver was turned on. After that, for each configuration, 20 sets of data that are equally spaced in time were collected and labeled as T1-T20. Comparison on each configuration was done to determine the effects of stack geometry.

In order to investigate the effects of stack separation gap, h, on velocity profile of thermoacoustic phenomena, results from configuration A were compared with results obtained from configuration B. The time interval for both configurations is the same. In this comparison, the time interval used is T7. The oscillating flow parameters for configuration A and B at time interval T7 is shown in Table 2. Value for viscous penetration depth, δ_v was calculated from [8][9],

$$\delta_v = \sqrt{\frac{2v}{\omega}} \tag{1}$$

with ω being the angular frequency of the sound wave ($1/f$) and v the kinematic viscosity of air (at room temperature and atmospheric pressure, $v = 1.6 \times 10^{-5}$ m^{2}s^{-1}). The viscous penetration depth describes the thickness of the layer of fluid around the stack plates that is restrained in its movement under the influence of viscous forces. As for the Reynolds number, Re_d it was defined as [5][7],

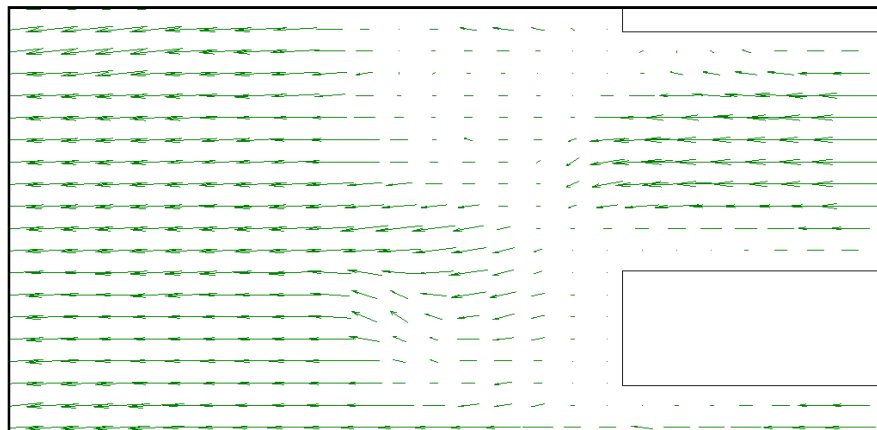$$\text{Re}_d = \sqrt{\frac{ut}{v}} \tag{2}$$

where u is the velocity at the end of the stack. Fig 2 shows the comparison of velocity profile at T7 for configuration A and B.

Table 2 : Oscillating flow parameters for configuration A and B at T7.

	u (m/s)	h/δ_v	Re_d
Configuration A	2.33	6.2664	145.625
Configuration B	2.36	18.7993	147.500
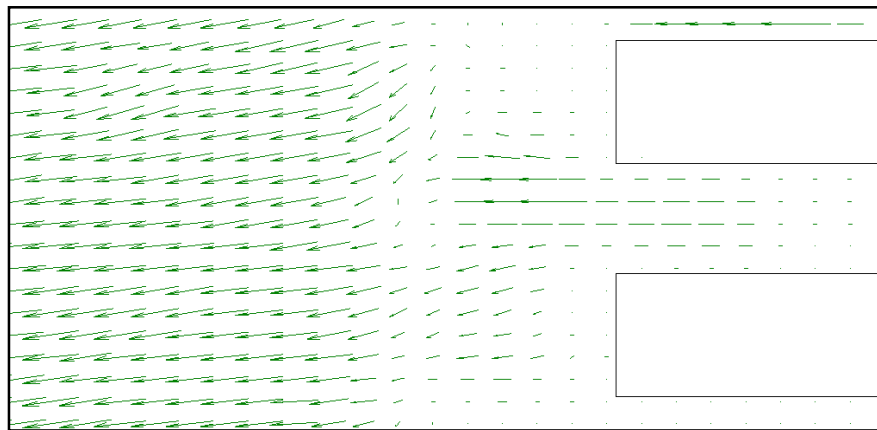
(a) Configuration A : $t = 1$ mm, $h = 1$ mm

(b) Configuration B : $t = 1$ mm, $h = 3$ mm

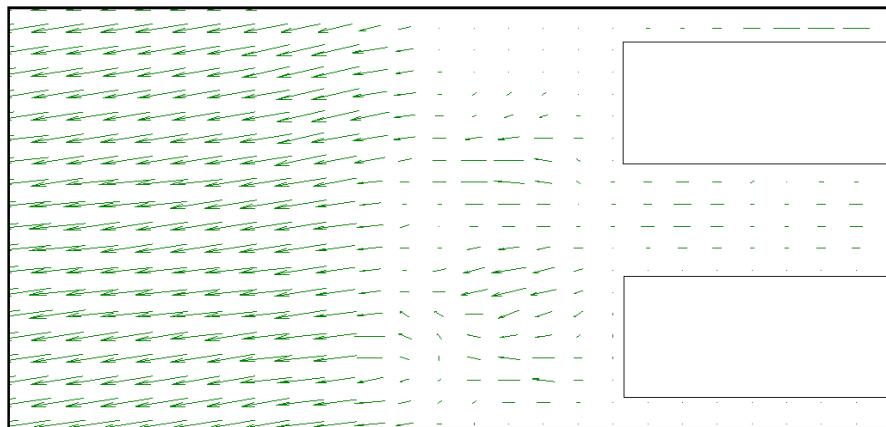Figure 2 : Comparison of velocity profile at T7 between configuration A and B.

Both velocity profiles do not show any formation of well-defined vortices. This is because both configurations had the same thickness of plates. Table 2 shows that the Reynolds number for both configuration are almost equal, therefore the flow pattern is almost the same at the edge of the stack plates. Besides that, there were differences on flow pattern between the separation gaps of stack plates. For configuration A, the velocity vectors at the separation gap region are smaller compared to configuration B. These differences were occurring due to the ratio of h/δ_v for both configurations being not equal.

From Table 2, we can see that the ratio of h/δ_v for configuration B is higher than A. Meanwhile, from the definition of δ_v, there were more particles that can move freely which are not influenced by the viscous forces for configuration B compared to configuration A.

Results from configuration A were compared with results from configuration C to study the effects of stack thickness, *t* on flow of thermoacoustics. For configuration A, the thickness of each stack plate is 1 mm while for configuration B is three times larger than that of A. The time interval T1 was used for this comparison and the oscillating flow parameters were shown in Table 3. Fig. 3 shows the comparison of velocity profile at T1 for configurations A and C, respectively.

Table 3 : Oscillating flow parameters for configuration A and C at T1.

	u (m/s)	h/δ_v	Re_d
Configuration A	2.45	6.2664	153.125
Configuration C	1.88	6.2664	352.500

(a) Configuration A : *t* = 1 mm, *h* = 1 mm
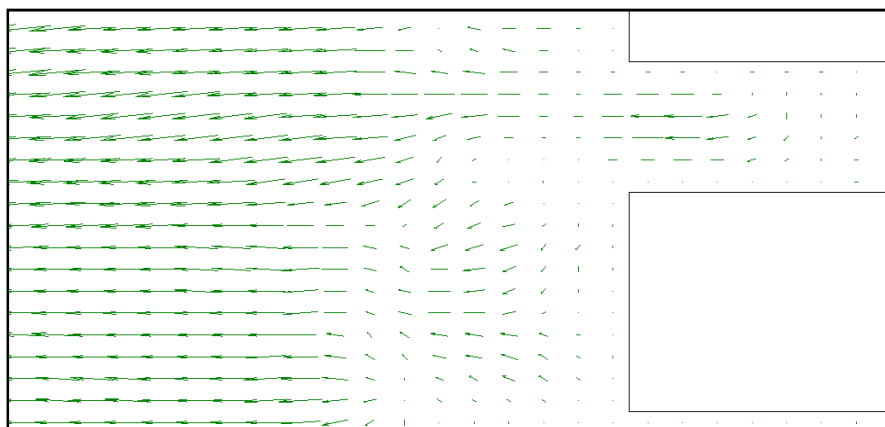
(b) Configuration C : *t* = 3 mm, *h* = 1 mm

Figure 3 : Comparison of velocity profile at T1 between configuration A and C.

The velocity vectors are relatively smaller near the edge compared to the region far from the stack plates. A vortex was observed near the edge of the plate in configuration C. Meanwhile, there were no clear vortices seen near the stack in

configuration A. The Reynolds number shown in Table 3 for configuration C is double the value for configuration A which explains the observed vortex in configuration C.

The above observations confirmed that the stack thickness has to be as thin as possible with the separation gap between $2\delta_k$ to $4\delta_k$ [8]. This study and previous studies completed with PIV have yet to look at the actual velocity profiles for separation gaps less than $2\delta_k$ and thinner plates due to the constraints associated with a PIV set-up. Stack heating and cooling in actual thermoacoustic systems have not been investigated due to the same reason too. However, with rapid advancement in the development of non-intrusive experimental techniques and reliable and repetitive experiments, the relationship between vortex generation, progression, and their significance, in the particle-plate conductive heat transfer can be better understood to promote the desired thermoacoustic effects.

4.0   CONCLUSION

Particle Image Velocimetry (PIV) was used to visualize the flow field at the end of the stack plates. The flow around three stack configurations at different geometry was measured and the effects of this geometry were determined by comparison between these configurations. The experimental findings are summarized as follows:

1) The flow velocity at the center of the separation gap increases as the separation gap increases
2) Vortices are observed at the edge stack plates when the thickness of the stack plates increase.

The above observations confirmed that the stack thickness has to be as thin as possible with the separation gap between $2\delta_k$ to $4\delta_k$. The non-intrusive PIV experimental technique has shown the relationship between vortex presence and its significance in relation with the plate separation and thickness. These are important factors in the particle-plate conductive heat transfer to promote the desired thermoacoustic effects.

ACKNOWLEDGEMENTS

REFERENCES

1. Carter, R. L., White, M., Steele, A. M. (1962). Private communication of Atomics International Division of North American Aviation Inc.
2. Herman, C., Kang, E., Wetzel, M. (1998). Expanding the Applications of Holographic Interferometry to the Quantitative Visualization of Oscillatory Thermofluid Processes Using Temperature as Tracer. *Exp. Fluids.* 24, 431-446.
3. Taylor, K. J. (1976). Absolute Measurement of Acoustic Particle Velocity. *J. Acoust. Soc. Am.* 59(3), 691-694.
4. Bailet, H., Lotton, P., Bruneau, M., Gusev. V., Valiere, J. C., Gazembel, B. (2000). Acoustic Power Flow Measurement in a Thermoacoustic Resonator by Means of Laser Doppler Anemometry (L.D.A) and Microphonic Measurement. *Appl. Acoust.* 60(1), 1-11.
5. Blance-Benon, P., Besnoin, E., Knio, O. (2003). Experimental and Computational Visualization of the Flow Field in a Thermoacoustic Stack. *C. R. Mecanique.* 331, 17-24.

6. Mao, X., Marx, D., Jaworski, A. J. (2005). PIV Measurement of Coherent Structures and Turbulence Created by an Oscillating Flow at the End of a Thermoacoustic Stack. *Proceeding of the iTi conference in turbulence.* 25-28 September. Bad-Zwishenahn, German.

7. Shi, L., Yu, Z., Jaworski, A. J., Abduljalil, A. S. (2009). Vortex Shedding at the End of Parallel-plate Thermoacoustic Stack in the Oscillatory Flow Condition. *World Academy of Science, Engineering and Technology.* 49.

8. Swift, G. W. (1988). Thermoacoustic Engines. *J. Acoust. Soc. Am.* 84, 1145-1179.

9. Berson, A., Michard, M., Blance-Benon, P. (2008). Measurement of acoustic velocity in the stack of a thermoacoustic refrigerator using particle image velocimetry. *Heat Mass Transfer.* 44, 1015-1023.